Article

Cell Reports

GABA-A Inhibition Shapes the Spatial and Temporal Response Properties of Purkinje Cells in the Macaque Cerebellum

Graphical Abstract

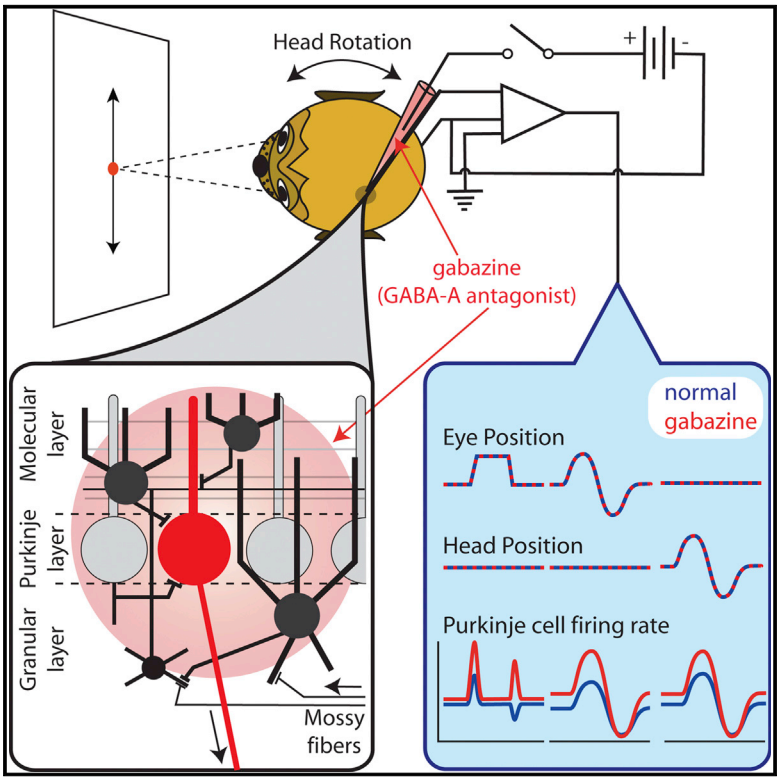

Highlights

- We studied the role of GABA-A inhibition on Purkinje cell responses in alert primates
- Gabazine disrupts local signal processing, but not efference copy signals or behavior
- Purkinje cell responsiveness, gain, and preferred direction are modulated by inhibition
- VPFL Purkinje cell eye and head velocity sensitivity is regulated by inhibition

Authors

Pablo M. Blazquez, Tatyana A. Yakusheva

Correspondence

pablo@pcg.wustl.edu

In Brief

The computations carried out by cerebellar cortex inhibitory interneurons in the awake animal are poorly understood. Blazquez et al. recorded macaque PCs while blocking GABA-A transmission near the recorded PC and demonstrate that inhibition plays an essential role in shaping the spatial and temporal response properties of cerebellar output neurons.

Blazquez & Yakusheva, 2015, Cell Reports *11*, 1043–1053
May 19, 2015
http://dx.doi.org/10.1016/j.celrep.2015.04.020

CellPress

Cell Reports
Article

GABA-A Inhibition Shapes the Spatial and Temporal Response Properties of Purkinje Cells in the Macaque Cerebellum

Pablo M. Blazquez[1,*] and Tatyana A. Yakusheva[1]
[1]Department of Otolaryngology, Washington University School of Medicine, 4566 Scott Avenue, St. Louis, MO 63110, USA
*Correspondence: pablo@pcg.wustl.edu
http://dx.doi.org/10.1016/j.celrep.2015.04.020

SUMMARY

Data from in vitro and anesthetized preparations indicate that inhibition plays a major role in cerebellar cortex function. We investigated the role of GABA-A inhibition in the macaque cerebellar ventral-paraflocculus while animals performed oculomotor behaviors that are known to engage the circuit. We recorded Purkinje cell responses to these behaviors with and without application of gabazine, a GABA-A receptor antagonist, near the recorded neuron. Gabazine increased the neuronal responsiveness to saccades in all directions and the neuronal gain to VOR cancellation and pursuit, most significantly the eye and head velocity sensitivity. L-glutamate application indicated that these changes were not the consequence of increases in baseline firing rate. Importantly, gabazine did not affect behavior or efference copy, suggesting that only local computations were disrupted. Our data, collected while the cerebellum performs behaviorally relevant computations, indicate that inhibition is a potent regulatory mechanism for the control of input-output gain and spatial tuning in the cerebellar cortex.

INTRODUCTION

Inhibition is ubiquitous in the cerebellar cortex, where all interneurons with the exception of granule and unipolar brush cells are inhibitory. Evidence from in vitro and anesthetized preparations suggests that GABAergic inhibition plays a key role in the computations carried out by the cerebellar cortex. For example, application of bicuculline, a potent GABA-A antagonist, disrupts the normal pattern of activation in cerebellar cortex following electrical stimulation of parallel fibers or the vibrissal pads (Gao et al., 2006). Tonic and spillover inhibition regulates the number of granule cells responsive to mossy fiber inputs and modulates the gain (slope of input-output relationship) of granule cells (Mitchell and Silver, 2003).

A critical aspect of cerebellar cortex function is its role in motor learning (Eccles et al., 1967). Traditionally, cerebellar learning has been associated with LTD and LTP at the parallel fiber to Purkinje cell (PC) synapse (De Zeeuw et al., 1998; Schonewille et al., 2010); however, emerging evidence indicates that local inhibitory interneurons are also capable of LTP and LTD (Jirenhed et al., 2013; Jörntell and Ekerot, 2002). Indeed, the current view is that cerebellar learning involves plasticity at multiple sites within the cerebellar network (D'Angelo, 2014). For instance, changes in eye and head velocity sensitivity of PCs in the ventral paraflocculus (VPFL) following vestibulo-ocular reflex (VOR) learning (Lisberger, 1994) may be partially attributed to changes in the excitability of inhibitory interneurons.

To understand the role of inhibition in cerebellar cortex function, it is imperative to study inhibition in the behaving animal; i.e., while the cerebellar circuit performs behaviorally relevant computations. Here, we studied the effect of blocking GABA-A receptors on the response of PCs in the macaque VPFL during oculomotor behaviors. The VPFL participates in the generation of eye movements during visual-vestibular stimulation (Rambold et al., 2002). VPFL mossy fiber inputs arriving from the brainstem carry efference copy, sensory information (retinal slip and vestibular), and perhaps proprioceptor information from extraocular muscles (Donaldson, 2000; Lisberger, 1994). VPFL PCs project to premotor neurons (Langer et al., 1985; Escudero et al., 1996; Lisberger, 1994). The strong efferent copy input to VPFL creates a powerful feedback loop (cerebellum-brainstem) that is responsible for the maintenance of pursuit behavior (Lisberger, 1994). Here, we blocked GABA-A receptors with SR95531 (gabazine), a potent GABA-A antagonist. Our results strongly suggest that GABA-A inhibition is necessary to confer the spatial response tuning and response gain of PCs and that regulation of inhibition could be a potent mechanism for cerebellar learning.

RESULTS

We investigated the role of inhibition in cerebellar cortex function by making minute injections of gabazine near a PC and evaluating how it affected the responses of the PC during oculomotor behavior. We first quantified the spread of drug in nervous tissue.

Spread of Gabazine in Tissue: Anesthetized Mouse

Figure 1A shows our experimental approach. We injected GABA pulses at the recording site, while measuring the neuronal response (i.e., decrease in activity following each GABA application). Next, we injected gabazine at a certain distance from the recording site. If the spread of gabazine overlaps with the region

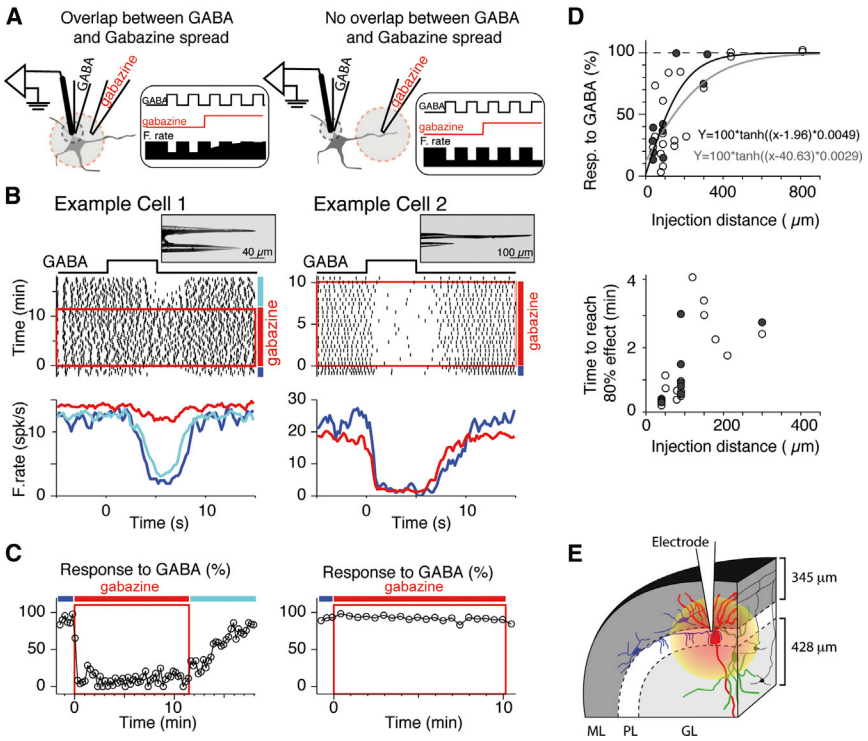

Figure 1. Spread of Gabazine in the Cerebellar Cortex of Mice

(A) Experimental approach used to measure the spread of drug in tissue. An injecting electrode delivered pulses of GABA at the recording site. Next, gabazine was injected using constant current through a second electrode located far from the recording site. Left and right panels show cartoons and the expected effects on firing rate (F.rate) when there was overlap between the spread of GABA and gabazine (left) and when there was no overlap (right).

(B) Example cells (left and right) recorded using the electrode configurations shown in pictures (insets on top). The distance between the gabazine injection and recording electrode tips was 40 and 440 μm for the example cells 1 and 2, respectively. In center, raster plot of spikes showing the neuronal response to pulses of GABA (+40 nA; 5 s duration). Time 0 on the x axis represents the onset of each GABA pulse, and time zero on the Y axes the onset of gabazine application. The red box indicates the period when gabazine was injected (+50 and +100 nA for example cells 1 and 2, respectively). For clarity, only one of every ten trials and one of every five trials are shown for example cells 1 and 2, respectively. In the bottom, average response to GABA pulses (includes all trials) before (blue), during (red), and after application of gabazine (cyan) are shown. Blue, red, and cyan lines indicate the periods before, during, and after gabazine application, respectively.

(C) Quantification of the response to pulses of GABA for the cells shown in (B). Each point represents the neuronal response to GABA in each of the trials shown in the raster: 0% corresponds to no changes in firing rate following GABA application and 100% corresponds to full inhibition following GABA application (no spikes). Blue, red, and cyan lines indicate the periods before, during, and after gabazine application, respectively.

(D) Population summary. Each dot represents data from a single neuron. (Top) The average response to GABA (%) during the last minute of gabazine injection (includes several GABA pulses; see C) versus distance between recording and gabazine injection site is shown. Bottom, time to reach 80% of gabazine effect, calculated using a fitting function over the data shown in (C) (see Experimental Procedures) versus distance between recording and gabazine injection sites. Filled circles and black fitting line represent the data obtained using +50 nA injection of gabazine, and empty circles and gray fitting line represent data obtained using +100 nA injection of gabazine.

(E) Cartoon that illustrates the area affected by gabazine application in the macaque VPFL. Purkinje cell (PC), molecular layer interneurons, Golgi cells, and granule cells are in red, blue, green, and black, respectively. GL, granular layer; ML, molecular layer; PL, PC layer. The thickness of ML and GL were estimated using the atlas of Paxinos et al. (2000).

affected by GABA (Figure 1A, left), the neuronal responses to GABA pulses would decrease during gabazine application. However, if there is no overlap (Figure 1A, right), there would be little or no effect on the neuronal response to GABA. Importantly, GABA does not spread far in tissue when using standard iontophoretic techniques (<20 μm; Herz et al., 1969).

We built electrode assemblies consisting of a single capillary glass glued to a three-barrel carbon fiber electrode (see photographs in Figure 1B). The capillary glass contained gabazine (10 mM; in 0.16 M NaCl [pH 4.0]). The three-barrel electrode contained a carbon fiber (5 μm thick) in one barrel, GABA (200 mM in distilled water) in a second barrel, and NaCl (160 mM) for current compensation in the third barrel. Figures 1B, left, and 1C, left show the response of a cerebellar cortex neuron recorded with an electrode assembly built with a separation of 40 μm between the tip of the multibarrel electrode and the tip of the capillary glass. For this neuron, injection of gabazine (+50 nA) cancelled the neuronal response to GABA within the first minute of gabazine injection. The neuron shown in Figures 1B, right, and 1C, right, which was recorded using an electrode assembly with separation of 440 μm, did not modify its response to GABA pulses during gabazine application (+100 nA). This indicates that the volume of tissue affected by gabazine did not overlap with the region near the recording electrode.

We recorded 31 neurons from the cerebellar cortex of eight adult mice using various assembly spacings. The effect of gabazine application on the neuronal responses to GABA decreased as the separation between the recording site and the gabazine injecting site increased (Figure 1D, top). Injection currents of +100 nA produced larger spread of gabazine than injection currents of +50 nA (filled and empty symbols in Figure 1D, top). Gabazine had an almost immediate effect on the neuronal response to GABA for separation distances smaller than 50 μm. For larger separation distances, the effect, if any, could take up to 4 min before reaching near-asymptotic values (>80% of full effect on responses to GABA pulses; Figure 2D, bottom). The effective spread of gabazine in brain tissue using our delivery method was reduced by more than 80% for

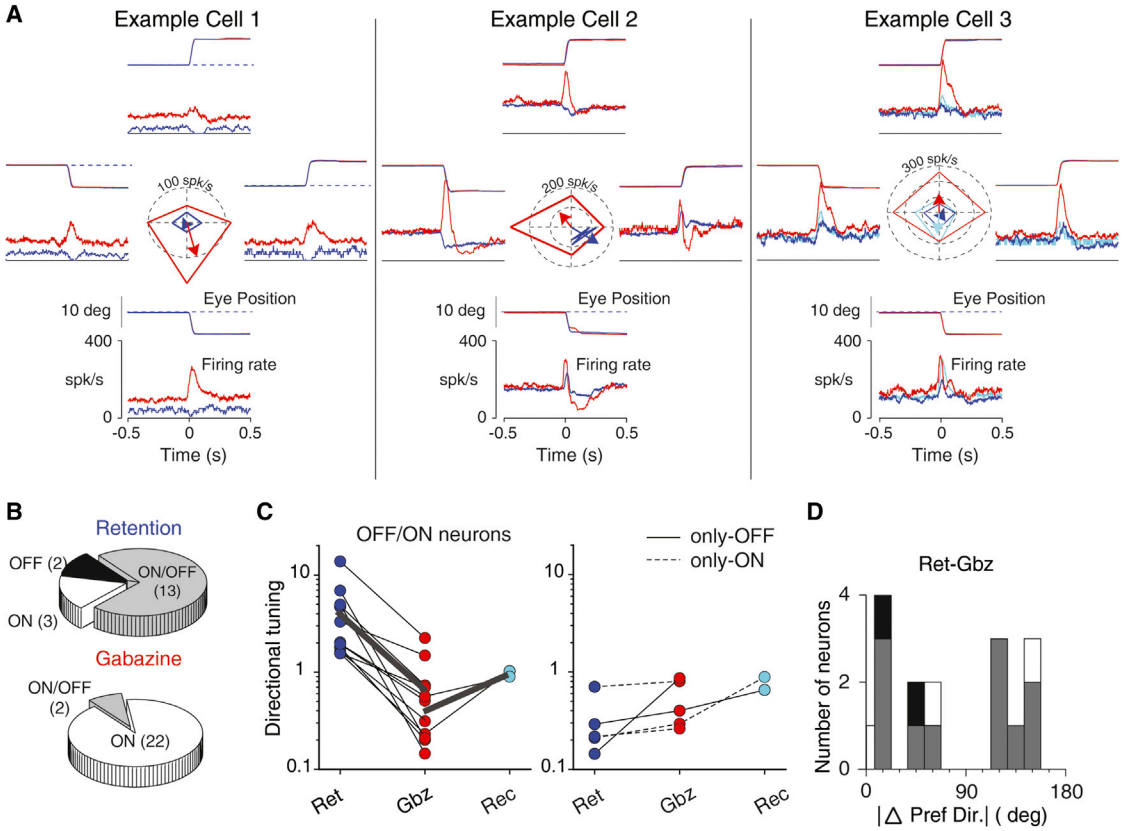

Figure 2. Response of VPFL PCs during Saccades with and without Gabazine Application

(A) Response of three example PCs to saccade before and during gabazine application. Each panel shows the average eye position (deg) and neuronal response (spk/s) during upward (top), downward (bottom), leftward (left), and rightward (right) saccades. Blue traces show data collected before drug application (retention period), red traces data collected during gabazine application (injection period), and cyan trace data collected after gabazine application (recovery period). Note that all types of PCs: OFF (cell1), OFF/ON (cell2), and ON (cell 3) become ON-only after gabazine injections (see also Figures S2 and S3).

(B) Distribution of saccade response types in VPFL PCs during retention and injection periods.

(C) Changes in the directional tuning of individual PCs with gabazine application. Only cells recorded during at least two periods are illustrated. Following the color code in (A), blue, red, and cyan show data collected during the retention (Ret), injection (Gbz), and recovery (Rec) periods, respectively. Thin black lines join data collected from the same neuron, and thick gray lines show the average from the corresponding neurons.

(D) Histogram showing the absolute differences in preferred direction of PCs recorded with and without drug application.

See also Figure S2.

separation distances larger than 230 and 420 μm when using gabazine injection current injection of +50 and +100 nA, respectively. Additionally, for any given cell that showed changes in its response to GABA application during gabazine injection, the effect of gabazine approached plateau (> 90%) within the first 4 min of injection.

Next, we present data collected in the macaque VPFL using injection currents of +50 nA. We use the above data obtained in mouse cerebellar tissue as proxy for the spread of gabazine in our macaque experiments because (1) our macaque electrodes had tip sizes similar to those used to measure the spread of gabazine in mice brain tissue (about 1- to 3-μm opening; see Inagaki et al., 2009); (2) the three layers of the cerebellar cortex are morphological and neurochemically identical in mammals (Eccles et al., 1967); and (3) the effective spread of gabazine was lower than the average thickness of the molecular and granular layers of mouse lobe IV–VI (0–1 mm lateral to the midline; mean of 300 and 270 μm, respectively; atlas of Franklin and Paxinos, 2008) and monkey VPFL (mean of 345 and 428 μm, respectively; atlas of Paxinos et al., 2000). For all the above, we argue that the effective spread of gabazine in our macaque experiments covered about two thirds of the molecular layer and about half of the granule cell layer (Figure 1E).

Gabazine Application Increases PC Burst Responses to Saccades and Eliminates or Inverts Inhibitory Responses

VPFL PCs respond to saccadic eye movements with increases in firing rate, decreases in firing rate, or both (named here as ON responses, OFF responses, and ON/OFF responses, respectively [see Experimental Procedures]). In our control PC population recorded using tungsten electrodes (n = 70), most PCs were ON/OFF neurons (63%; n = 44/70; Figure S1), and the average maximum and minimum saccade response amplitude was 70.8 and −32.4 spk/s, respectively. This indicates that, as a population, VPFL PCs show ON/OFF saccade responses.

Figure 2A shows the response of three example PCs recorded during retention (blue traces) and injection (red traces) of gabazine (see also Figure S2). These PCs were classified as OFF (left), ON/OFF (center), and ON (right) neurons based on their response to saccades during the retention period. Interestingly, during gabazine application, all three neurons changed to ON neurons. Perhaps the most remarkable change is that of example cells 1 and 2, where saccade directions that generated clear OFF responses during the retention period switched to strong ON responses during gabazine application. Furthermore, all three example neurons changed their directional preference with gabazine application (compare the direction of the blue and red arrows at the center graph). The cell shown to the right was also recorded during the recovery period (cyan). During the recovery period, the burst associated with saccades decreased, although it remained larger than that observed during the retention period.

Most PCs recorded during the retention period were ON/OFF neurons (72%; 13/18; Figure 2B, top pie chart); however, most PCs recorded during the injection period were ON neurons (92%; 22/24; Figure 2C, bottom pie chart). The maximum neuronal response increased about 61.4% during gabazine application (mean; 119 versus 192.1 spk/s for retention versus injection periods, respectively), whereas the minimal response amplitude took positive values during the injection period (−35.1 versus 94.7 spk/s for retention versus injection periods, respectively). The directional tuning of the neuronal response decreased during gabazine application for all neurons classified as ON/OFF during the retention period ($n = 9$; $p = 0.003$; Wilcoxon sign rank test; Figure 2C, left) and tended to increase during the recovery period ($n = 2$). The decrease in the neuronal tuning was accompanied by an increase in the tuning width (mean; 36.2 versus 110.2 spk/s for retention and injection periods, respectively; $p = 0.0099$; Wilcoxon sign rank test; see also Experimental Procedures and Figure S1). We found no changes, or increases, in spatial tuning for ON and OFF neurons (Figure 2D, right, albeit the low n). Lastly, as shown in Figure 2A for the example neurons, gabazine application changed the saccade preferred direction of PCs; often the preferred direction shifted near 180 degrees (Figure 2D and see center polar graphs in Figure 2A) but has no consistent effect in the neuronal response latency ($p = 0.34$; Wilcoxon rank test).

Importantly, microinjections of gabazine at the current and concentration used in this study had no effect on saccade latencies and position errors (Figure S3; ANOVA; $p >> 0.05$).

Gabazine Increases PC Responses to Pursuit and VOR Cancellation

The canonical VPFL PC carries ipsilateral or down eye velocity information and ipsilateral or down head velocity information (Blazquez et al., 2003; Lisberger, 1994). Figure 3 shows an example PC recorded during sinusoidal pursuit (A) and VOR cancellation (B) before, during, and after gabazine application (blue, red, and cyan, respectively). Gabazine injection increased the amplitude of modulation for both pursuit and VOR cancellation (from 40.4 to 64 spk/s for pursuit and from 11.6 to 27.8 spk/s for VOR cancellation), with small changes in phase (from 24.4 to 15.8 deg for pursuit with respect to eye velocity and from −8 to +10.9 deg for VOR cancellation with respect to head velocity). During the recovery period, the neuronal modulation during pursuit decreased toward preinjection values (49 spk/s).

Figures 3C and 3D illustrate the population data. The neuronal response amplitude for pursuit was larger during the injection period than during the retention period (mean ± SD; 64.9 ± 24 versus 42.2 ± 14 spk/s; $p = 0.01$; Mann-Whitney U test) and larger than that found with tungsten electrode recordings (31.46 ± 12.6 spk/s; $p = 0.00003$; Mann-Whitney U test; Figure 3C, left). This change was significant in cell-by-cell comparisons ($p = 0.025$; Wilcoxon sign rank test; Figure 3C, right). Similar results were found for PCs recorded during VOR cancellation. PCs increased their amplitude of modulation with gabazine application (17.2 ± 13.4 [$n = 31$], 13.4 ± 8.9 [$n = 8$], and 25.4 ± 12.7 [$n = 6$] spk/s for the tungsten, retention, and injection population, respectively). These changes showed marginal significance, perhaps due to the low n ($p = 0.043$ and $p = 0.046$ for gabazine versus tungsten and gabazine versus retention population, respectively; Mann-Whitney U test; Figure 3D left). Moreover, the four cells recorded during both periods, retention and gabazine injection, increased the modulation with gabazine application (Figure 3D, right). In summary, we found that gabazine application increased the amplitude of modulation during pursuit and VOR cancellation by 66.5% ($n = 8$) and 70.6% ($n = 4$), respectively. When modulation is expressed as sensitivities, we observed an increase in eye velocity sensitivity (mean; 1.8 versus 2.7 spk/s/deg/s [retention versus gabazine]; $p = 0.036$; Wilcoxon rank test) and, marginally, head velocity sensitivity (mean; 0.77 versus 0.21 spk/s/deg/s [retention versus gabazine]; $p = 0.068$; probably because the low n; Wilcoxon rank test). There were no changes in the neuronal response phase ($p > 0.24$; Wilcoxon rank test; Figure S4). Remarkably, although the neuronal responses to pursuit in the preferred orientation (i.e., horizontal or vertical) increased, the neuronal responses to pursuit in the non-preferred orientation (i.e., vertical or horizontal) were not affected by gabazine application (Figure 3E; $n = 7$; $p = 0.75$; Wilcoxon rank test; Figure S5).

To measure eye position and eye-acceleration-related neuronal discharge, we studied the neuronal responses to step ramp pursuit toward the neuronal preferred direction. The two example neurons in Figure 4A showed a clear increase in their response during gabazine application, which could be described in terms of changes in neuronal sensitivities to eye movement parameters. Individual neurons recorded with gabazine application tended to increase their eye position, eye velocity, and eye acceleration sensitivities, although this was significant only for the eye velocity component (Figure 4B, bottom; $p < 0.003$; Wilcoxon sign rank test). The same was true at the population level; eye position, velocity, and acceleration sensitivities increased with gabazine application, but only increases in eye velocity sensitivity were significant ($p < 0.0002$; Mann-Whitney U test; Figure 4B).

Microinjections of gabazine at the current and concentration used in this study had no effect on pursuit behavior (latency and velocity error; Figure S6; ANOVA; $p >> 0.05$).

Gabazine Has No Effect on the Efference Copy of Motor Commands

A large proportion of mossy fibers entering the VPFL provide an efference copy of the motor command to the cerebellar cortex.

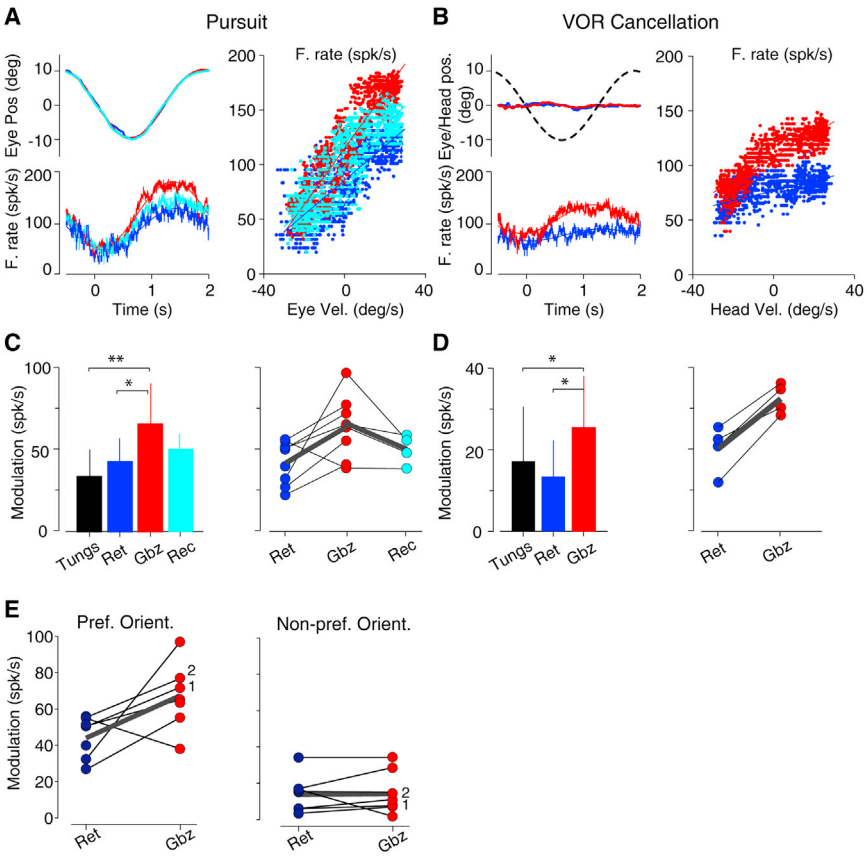

Figure 3. Response of VPFL PCs during Sinusoidal Pursuit and VOR Cancellation with and without Gabazine Application

(A) Response to pursuit of an example VPFL PC recorded before (blue), during (red), and after (cyan) gabazine application. Left: top traces show the eye position and bottom traces the neuronal response. Right: firing rate (F.rate; spk/s) is plotted versus eye velocity (Eye Vel.; deg/s).

(B) Response to VOR cancellation of an example VPFL PC recorded before (blue) and during (red) gabazine application. Left: top traces show the behavioral response and table position (black dashed line). Left: bottom traces show the neuronal response. Right: firing rate (spk/s) is plotted versus head velocity (Head Vel.; deg/s).

(C) Left: bar graph illustrating the population data recorded during sinusoidal pursuit. Right: single-cell data collected during more than one period. Retention (blue; Ret), injection (red; Gbz), and recovery (cyan; Rec) periods are shown. Thin black lines join data collected from the same neuron, and thick gray lines show the average from the corresponding neurons. Asterisks indicate significance (*0.05 < p < 0.01 and **p < 0.01). Data are represented as mean ± SD. Abbreviations: Ret, Gbz, and Rec, population recorded with multibarrels electrodes during the retention, injection, and recovery periods, respectively; Tungs, population recorded with tungsten electrodes.

(D) Same as (C) but for VOR cancellation.

(E) Comparison of the amplitude of modulation of PCs during sinusoidal pursuit in the preferred (left) and non-preferred (right) orientations. Only neurons recorded during vertical and horizontal sinusoidal pursuit with and without gabazine application are shown. Black thin lines connect data from the same neuron. Thick gray lines show the average from the corresponding neurons. Numbers 1 and 2 indicate the example neurons shown in Figure S5.

See also Figure S5.

This signal is used to help maintain pursuit and generate predictions of the current motor state (Ghasia et al., 2008). To investigate whether gabazine injections affect the efference copy signal, we compared the responses of eye-movement-related mossy fibers, which are thought to carry the efference copy signal of the eye movement, with and without gabazine application. Figure 5A shows an example mossy fiber recorded during spontaneous eye movements (see Experimental Procedures, [Heine et al., 2010], and [Laurens et al., 2013] for a description of how to identify mossy fibers). The eye position sensitivity of this mossy fiber, calculated as the slope of the fitting line relating mean eye position during fixation and mean firing rate, did not change during gabazine injection (slopes of blue versus red lines in Figure 5A, right). This was true for all recorded mossy fibers (n = 4; Figure 5B), suggesting that the efference copy pathway was not affected by our experimental manipulation. Note that, during pursuit of a laser in the dark, the efferent copy information is arguably the major signal driving the response of VPFL PCs because retinal slip is minimal, and the macaque oculomotor system notably lacks proprioreceptors typically found in skeletal musculature (i.e., muscle spindles; Ruskell, 1999). Moreover, the response profile of the mossy fibers shown here resembles that of prepositus hypoglossi neurons, a major source of efferent copy signal to VPFL (Escudero et al., 1996).

Gabazine Increases PC Simple Spike Discharge but Does Not Affect the Spike Regularity or the Complex Spike Discharge

We found no differences in DC firing rate, calculated as the mean firing rate during center fixation, between PCs recorded with tungsten electrodes (n = 120) and multibarrel electrodes during the retention period (n = 13; p > 0.084; Mann-Whitney U test; Figure 6A, left). However, DC firing rate increased during gabazine injection (n = 13 retention versus n = 11 injection; mean ± SD; 74 ± 26.3 versus 102.6 ± 30.7 spk/s; p = 0.0075; Mann-Whitney U test; Figure 6A, left). This difference became more pronounced when comparisons were made in a cell-by-cell basis (p = 0.0037; Wilcoxon sign rank test; Figure 6A, right). During the recovery period, the DC firing rate decreased relative to the injection period (126 ± 26 and 101 ± 18 spk/s, respectively; p = 0.043 Wilcoxon sign rank test; Figure 6A, right). The CV2 was not affected by gabazine injection (p = 0.155; Wilcoxon sign rank test; Figure 6B), indicating that there was no effect on spike regularity.

Injection of gabazine did not affect the DC firing rate or CV2 of complex spike discharge (Figures 6C and 6D; p = 0.86 and p = 0.62 for DC firing rate and CV2, respectively; Mann-Whitney U test; Figures 6C and 7D, left panels). This was also true at the individual cell level (p = 0.74 and p = 0.49 for DC firing rate and

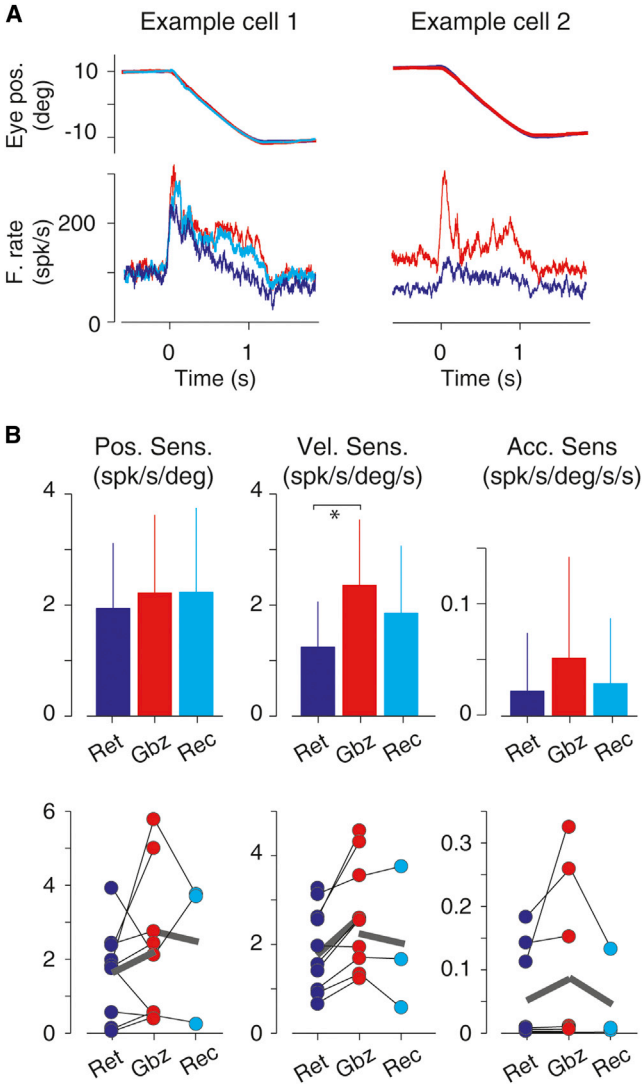

Figure 4. Response of VPFL PCs during Step Ramp Pursuit with and without Gabazine Application

(A) Response of two example VPFL PCs recorded before (blue), during (red), and after (cyan in example cell 1) gabazine application. Top traces show the behavioral responses (deg) and bottom traces the neuronal responses (spk/s). (B) Top panels show bar graphs illustrating the changes in eye position, velocity, and acceleration sensitivity of the population data (left, center, and right, respectively). Bottom panels show data from individual cells. Retention (blue; Ret), injection (red; Gbz), and recovery (cyan; Rec) periods are shown. Thin black lines join data collected from the same neuron, and thick gray lines show the average from the corresponding neurons. Asterisk indicates significance (*0.05 < p < 0.01). Vertical bars correspond to SDs.
See also Figure S6.

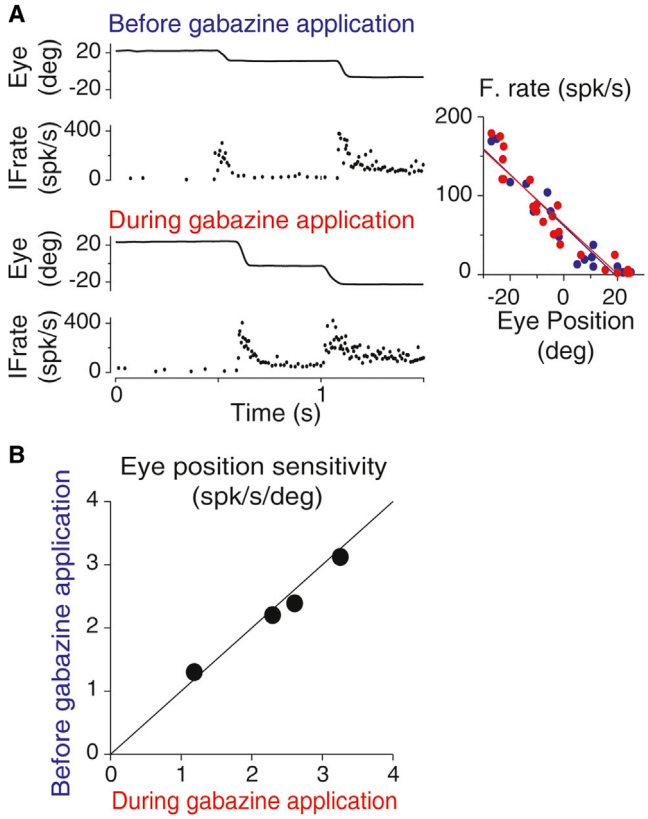

Figure 5. Gabazine Application Does Not Affect the Efference Copy Information

(A) Example of instantaneous mossy fibers discharge (IFrate) during spontaneous eye movements (Eye, eye position). The top and bottom show the response of the same mossy fibers before and during gabazine injection, respectively. The right panel shows the method used to calculate the sensitivity of mossy fibers to eye position. The sensitivity corresponds to the slope of the fitting line (blue for data collected before gabazine application and red for data collected during gabazine application). Vertical bars correspond to SDs. (B) Sensitivity of each recorded mossy fiber (n = 4) before and during gabazine application.

CV2, respectively; Wilcoxon sign rank test; Figures 6C and 6D, right panels).

Changes in PC Responses during Gabazine Application Are Not due to Changes in Baseline Firing Rate

We used two methods to investigate whether the changes observed in PC response to pursuit and VOR cancellation during gabazine application could be a direct consequence of increasing the neuronal DC firing rate. First, we divided the PC population recorded with tungsten electrodes into three groups based on their DC firing rate (group I < 70 spk/s; group II 70–90 spk/s; group III > 90 spk/s). In all groups, the dominant type of saccade response corresponded to the ON/OFF type (58%, 66%, and 80% for groups I, II, and III, respectively), and there was no relation between amplitude of modulation during sinusoidal pursuit or VOR cancellation and DC firing rate (Figures S7A and S7B; $p > 0.24$ and $p > 0.85$ for pursuit and VOR cancellation, respectively; Mann-Whitney U test).

We recorded the responses of six PCs to sinusoidal pursuit before and during tonic application of L-glutamate. L-glutamate increased the DC firing rate in all six PCs (the more L-glutamate we injected, the larger the DC firing rate) but caused no consistent changes in the amplitude of modulation during pursuit (Figures 7A and 7B; see fitting lines for individual cells). Our data indicate that the response changes observed during

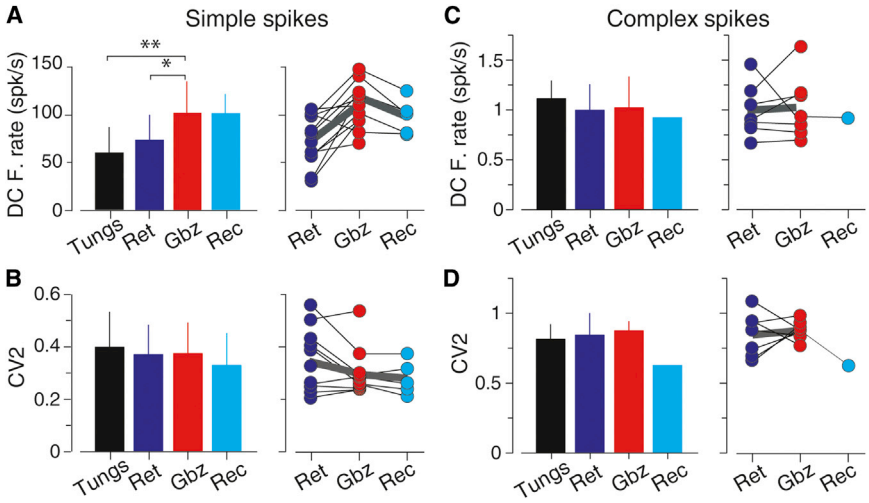

Figure 6. Effects of Gabazine Application on the Discharge Properties of VPFL PCs

(A) Left: comparison of simple spikes DC firing rate of VPFL PCs recorded with tungsten electrodes (black; Tungs) with multibarrel electrodes during the retention period (blue; Ret), injection period (red; Gbz), and recovery period (cyan; Rec). Right: data from single neurons recorded with multibarrel electrodes during the retention, injection, or recovery period. Only data recorded during at least two periods is shown. Thin black lines join data collected from the same neuron, and thick gray lines show the average from the corresponding neurons. Asterisks indicate significance (*0.05 < $p < 0.01$ and **$p < 0.01$).

(B) Same as (A) for CV2.

(C and D) Same as (A) and (B) for complex spikes.

gabazine application are not the result of increases in DC firing rate.

DISCUSSION

We investigated the role of GABA-A-receptor-mediated inhibition in the computations performed by the macaque VPFL using a finely targeted pharmacological and neurophysiological approach. Specifically, we compared the responses of VPFL PCs in alert primates during oculomotor behaviors before and during application of minute amounts of gabazine. Our drug application only affected processes or signal transformations taking place within a small volume of the cerebellar cortex because (1) the effective spread of the drug was less than 250 μm (Figure 1) and (2) the efference copy of the eye movement, a major input signal to VPFL, did not change with drug application. We found that gabazine increased the response amplitude of PCs to saccades, changed their directional preference, and decreased their spatial tuning. We also found that gabazine increased the neuronal response to pursuit and VOR cancellation. Our results suggest that GABA-A inhibition is an important mechanism to regulate the gain and directional preference of cerebellar cortical output neurons.

Characteristics of the Experimental Manipulation

The effective spread of gabazine was less than the average thickness of the VPFL molecular and granular layers and corresponds to less than 1% of the total volume of the structure (6–9 mm^3 folia V-X of the flocculus complex; Paxinos et al., 2000, Rambold et al., 2002). Functionally, the VPFL is divided into three sagittal zones: two related to vertical eye movements and one related to horizontal eye movements (Sato and Kawasaki, 1990). These zones project to different areas of the vestibular nuclei and receive inputs from different portions of the inferior olive (Sato and Kawasaki, 1991). Our gabazine application did not modify the information carried by mossy fibers (efference copy and proprioceptive pathways) nor the activity of the olivocerebellar pathway (complex spikes), suggesting that we affected only local computations.

Because our drug application does not target specific cell types, our data cannot provide insights into the mechanisms or neuronal types responsible for the changes in PC responses demonstrated here. However, the data demonstrate that regulation of inhibition shapes PC responses in the alert animal.

Potential Role of GABA-A Inhibition in VPFL Function: Saccades

Saccade-related signals are strong in the VPFL (Miles et al., 1980) and can be used to maintain saccade accuracy (Noda and Suzuki, 1979) and to update internal models of the eye movement (Ghasia et al., 2008). Gabazine changed the saccade response of PCs from only OFF and ON/OFF to only ON responses, suggesting that PCs receive omnidirectional ON saccade responses through the parallel fiber system (their only excitatory input) and that the directional preference of PCs is controlled by selective inhibition (Figure S7C). This view contrasts with computational modeling architectures that assume that VPFL PCs in the vertical and horizontal zones receive only vertical and horizontal eye-related information, respectively (Blazquez et al., 2003; Lisberger, 1994). However, our data are in agreement with the anatomy of the circuitry, where parasagittally organized parallel fibers functionally link different zones of the VPFL (Eccles et al., 1967). Selective inhibitory control would be best carried out by nearby molecular layer interneurons (stellate and basket cells) because they receive inputs from the same parallel fibers than the recorded PC (Eccles et al., 1967). A large portion of the inhibitory control to PCs from molecular layer interneurons is carried out by GABA transmission, although ephaptic transmission from basket cells to PC at the pinceau have also been described (Blot and Barbour, 2014). In addition, gabazine can have an indirect effect over the gain of PCs by changing the gain of their input elements (i.e., granule cells). In support, Duguid et al. (2012) showed that reduction of tonic inhibition increases the gain and saliency in granule cell responses to sensory stimulation. However, because VPFL mossy fibers contacting a single granule cell likely have similar preferred orientations as the PCs above (Cerminara et al., 2013; Pijpers et al., 2006; Sato and Kawasaki, 1990, 1991), it is unlikely that changes

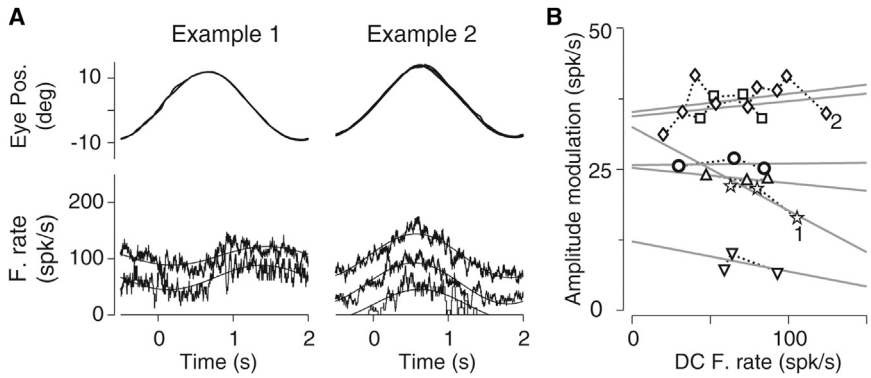

Figure 7. Effect of Increasing DC Firing with L-Glutamate on the Neuronal Response to Sinusoidal Pursuit

(A) Top: eye position. Bottom: neuronal firing rate. Example cell 1 (left) shows the response of a neuron while retaining (lower trace; +20 nA) and injecting (upper trace; −25 nA) L-glutamate. Example cell 2 (right) shows the response of a neuron while retaining (lower trace; +20 nA), and injecting (middle and upper trace; −20 and −60 nA, respectively) L-glutamate.

(B) Amplitude of modulation to sinusoidal pursuit versus DC firing rate for the six PCs recorded with L-glutamate injection. Different DC firing rate values were obtained for different L-glutamate current injections for each cell. Different symbols show data collected from different neurons. Dashed lines connected data from the same neuron. Straight lines show the fitting lines to data collected from individual neurons. Numbers 1 and 2 indicate example neurons 1 and 2, respectively.

See also Figure S7.

in granule responsiveness can cause the omnidirectional response of PCs to saccades.

Potential Role of GABA-A Inhibition in VPFL Function: Pursuit and VOR Cancellation

Gabazine increased the response of PCs to pursuit and VOR cancellation, suggesting that inhibition regulates the input/output relationship in cerebellar cortex. These increases are not due to changes in DC firing rate, as demonstrated by our injections of L-glutamate. We argue that gabazine increased PC gain by increasing the input/output relationship in granule cells (Duguid et al., 2012; Mitchell and Silver, 2003). Thus, GABA-A inhibition may work in conjunction with LTP/LTD in parallel fiber-PC synapses to support motor learning (Schonewille et al., 2010; Hansel et al., 2006; Jirenhed et al., 2013; Liu et al., 2008). Indeed, the parameters that underwent the larger changes with gabazine application were eye and head velocity sensitivities, which are the components believed to drive VOR motor learning (Blazquez et al., 2003; Lisberger, 1994). Regulation of inhibition could also explain the observation that mice lacking LTD at parallel fiber to PC synapses can adapt their VOR gain, albeit they require longer training times (van Alphen and De Zeeuw, 2002). Interestingly, gabazine increased the neuronal responsiveness to smooth pursuit only in the preferred orientation of the neuron. This can be explained by a reduction of inhibition in nearby granule cells, because, as mentioned above, reduction of inhibition in granule cells increases their input-output gain and the granule cells affected by gabazine would most likely have a similar preferred orientation as the recorded PC (Cerminara et al., 2013; Pijpers et al., 2006) (Figure S7D).

How can we reconcile the finding that gabazine changed the spatial response tuning of PCs during saccades, but not during pursuit? PCs receive saccade- and smooth-eye-movement-related inputs through the same set of mossy fibers (with a burst tonic response type, e.g., from prepositus hypoglossi; Miles et al., 1980; Escudero et al., 1996); hence, the effect must be specific to the type of neuronal activity associated with these behaviors. Saccades generate a powerful burst of activity in mossy fibers, whereas pursuit generates smaller changes in firing rate that build over longer time scales. It is possible that the subset of parallel fibers that form functional connections with each VPFL PC determines its eye movement preferred orientation, whereas the rest of mossy fibers form synapses with very high activation threshold (i.e., almost silent synapses; Isope and Barbour, 2002). Gabazine application may reduce the activation threshold just enough for these synapses to allow the high burst of activity associated with saccades to generate EPSCs in PCs, but not the smaller activity associated with pursuit. Alternatively, fast inhibitory transmission (e.g., GABA-A) could be responsible for the spatial tuning of PCs during saccades, whereas other forms of synaptic transmission (e.g., through GABA-B receptors) play the major role in shaping the directional tuning of PCs during pursuit. Perhaps the different effect of gabazine on PC responses to saccade and pursuit eye movements may reflect different cerebellar strategies to control ballistic (e.g., saccades) and smooth (e.g., pursuit) movements.

In conclusion, our experiments show evidence for a role of GABA-A inhibition in the spatio-temporal signal transformations carried out by the cerebellar cortex while the structure performs behaviorally relevant computations. Excitation is likely the main driver of PC responses during pursuit and VOR cancellation because gabazine did not remove but rather increased the eye velocity sensitivity. However, inhibition is a strong mechanism to regulate saccade responses because it can overpower the excitatory drive arriving through parallel fibers. These results can serve as a bridge to link the remarkable advances in our understanding of cerebellar physiology from in vitro and anesthetized preparations with the available data in the alert animal.

EXPERIMENTAL PROCEDURES

Animal Preparation and Recording Setup

Mouse

Eight adult C57BL/6 mice were anesthetized with xylazine (13 mg/kg every 2 hr). Following, a midline incision was made on the scalp to expose the bone surface. We removed 3 mm^2 of the occipital bone posterior to the lambdoid suture and the underlying dura mater to expose lobules IV, V, and VI of the cerebellar cortex, through which we run our electrode tracks. Animals were euthanized after the experiment with sodium pentobarbital (50 mg/kg). Surgical and experimental protocols were in accordance with

the NIH guidelines and approved by the Washington University Committee on Animal Care.

The mouse recording setup consisted of an AC differential amplifier (BAK Electronics), a hydraulic microdrive (Narishige), and a Neurophore BH-2 iontophoretic pump system (Medical Systems). Data were acquired using a Power 1401 (Cambridge Electronic Design) connected to a PC computer (Spike2 software; Cambridge Electronic Design).

Monkey

We used three macaques (M1, M2, and M3) of 5–7 years of age and 6–11 kg for neuronal recording in the VPFL. We used standard surgical procedures performed under isoflurane anesthesia and aseptic conditions in a fully equipped surgical suite (Heine et al., 2010). In a first surgery, we implanted a stainless steel head post for head fixation and an eye coil to monitor horizontal and vertical eye position. Two weeks later, we implanted a recording chamber aimed to the left VPFL. Surgical and experimental protocols were in accordance with the NIH guidelines and approved by the Washington University Committee on Animal Care.

The macaque recording setup consisted of an AC differential amplifier (BAK Electronics), a hydraulic microdrive (Trent Wells), a Neurophore BH-2 iontophoretic pump system (Medical Systems), and a search coil eye movement detector (C.N.C. Engineering). A Power 1401 (Cambridge Electronic Design) connected to a PC computer (Spike2 software; Cambridge Electronic Design) was used for data acquisition and stimulus presentation. A red laser projected on a white screen placed in front of the animal (48 cm) served as our main visual stimulus.

Training and Behavioral Paradigm

Macaques were trained to maintain their gaze on the laser using standard water restriction protocols. We used five tasks: (1) spontaneous eye movements in the light. This protocol was used to analyze the neuronal response to saccade eye movement when visually guided saccade data were not available. (2) Visually guided saccades to four cardinal directions. After an initial central fixation (1–1.7 s), the laser target was stepped 15 or 20 deg in one of four cardinal directions, where it remained stationary for 1 s. (3) Horizontal and vertical sinusoidal pursuit. The laser was moved sinusoidally around the center fixation at 0.4 Hz and 10 deg amplitude. (4) Vestibulo-ocular reflex (VOR) cancellation. Animals fixated a stationary target (red laser) while they were passively rotated along the earth vertical axis (yaw rotation) at 0.4 Hz and 10 deg amplitude; animals were rewarded with water each 1–1.5 s. (5) Step ramp pursuit to four cardinal directions. After an initial central fixation (1–1.5 s), the laser was moved toward the endpoint (10 deg from center) at a constant velocity (10 or 20 deg/s for 1.5 or 3 s, respectively). At the onset of pursuit, the target stepped back a few degrees to avoid catch-up saccades (Heine et al., 2010).

Carbon Fiber Multibarrel Electrode Preparation, Unit Recording, and Drug Application

Mouse

Electrode assemblies consisted of a single capillary glass electrode attached to a three-barrel carbon fiber electrode. Both the single capillary glass electrode and the three-barrel carbon fiber electrode were pulled using a horizontal puller (PML-107L; MicroData Instruments). The tip of the carbon fiber was etched by passing electric current through a saline bridge until it was reduced to about 10–15 μm (Inagaki et al., 2009). Next, we glued the multibarrel electrode to the single capillary glass electrode using dental cement with a separation between the tip of the capillary glass and the three-barrel electrode of 0.04–0.8 mm (see Figure 1, pictures on top right). Electrodes were inspected before and after recording to confirm that the integrity of the assembly and the size of the electrode tips were not compromised. One barrel of the three-barrel electrode was filled with GABA (500 mM in 0.165 M NaCl [pH 5.0]), a second barrel with 0.165 M NaCl for current compensation, and a third barrel contained the carbon fiber (5 μm). The capillary glass electrode was filled with gabazine (10 mM in 0.165 M NaCl [pH 3.5]).

Our electrode penetrations were limited to 2 mm deep from the surface of the cerebellum (throughout vermis lobules IV–VI). Once a spontaneously firing neuron was isolated, we tested the effect of GABA injection (+15 to +50 nA) while retaining gabazine (−50 to −100 nA). GABA was injected intermittently using pulses of 2–5 s duration every 10–30 s. The exact pulse parameters for GABA injection were chosen online and were tailored to each recorded neuron to consistently generate large decreases in firing rate (near full pauses) but allowing the cell to recover in between pulses. The first 3–10 pulses of GABA (before gabazine injection) were used as control responses. Following this, we injected gabazine (+50 or +100 nA constant current) for up to 10 min. Note that we continued delivering pulses of GABA while injecting gabazine (see Figure 1A).

Monkey

We used tungsten electrodes (FHC; 3–8 MOhms) and carbon fiber multibarrel electrodes. Carbon fiber multibarrel electrodes were made using procedures described elsewhere (Inagaki et al., 2009). Briefly, a carbon fiber (5–7 μm) was inserted into one barrel of a three- or four-barrel capillary glass, the glass ensemble was then pulled (PML 107L; MicroData Instruments), and the remaining barrels were filled with solution. One of the barrels was filled with 2 (3 carboxypropyl) 3 amino 6 methoxyphenyl pyridazinium bromide (gabazine; 10 mM in 0.165 M NaCl at pH 3; Sigma-Aldrich) or L-glutamate (20 mM in 32 mM NaOH; Sigma-Aldrich). Another barrel was filled with 0.165 mM NaCl solution for balance compensation. The values used for current retention and injection of gabazine were −50 to −75 nA (retention) and +50 to +75 nA (injection). For glutamate, these values were +15 to +75 nA (retention) and −10 to −50 nA (injection). Neuronal responses to gabazine application were measured after 30 s of the onset of gabazine application to guarantee that drug was present in the extracellular space. Similarly, neuronal responses during the recovery period were measured after 30 s of ending gabazine application. Often, this period was not sufficient to get full recovery as indicated by the fact that the DC firing rate was still higher than preinjection levels.

We identified the three layers of the VPFL and their neuronal elements based on their characteristic neuronal activity (Heine et al., 2010; Laurens et al., 2013). PCs were identified by the presence of simple and complex spikes. Often, complex spikes could be heard through the entire recording, but it was difficult to maintain isolation of both simple and complex spikes simultaneously for long periods. Mossy fibers were identified in the granular layer as units with narrow spikes (<0.25 ms duration) and monophasic profiles that could not be isolated for long distances (Laurens et al., 2013).

Analysis Methods

Data analysis was performed offline in Matlab 2007 (MathWorks).

Mouse

Neuronal responses to GABA during gabazine application were compared to those during the control period (before gabazine) to quantify the effective spread of drug in tissue. We built peristimulus time histograms (PSTH) of the neuronal firing rate aligned with the onset of pulses of GABA during the control period (see Figure 1B, blue lines). We used these PSTHs to manually select for each cell a time period that showed clear responses to GABA (decreases in firing rate); this is the response period. The same time period was used as the test period during injection of gabazine. Neuronal response to GABA (%) was measured for each pulse of GABA as

$$\text{Response to GABA}\ (\%) = 100 * \left(1 - \frac{FR_{RP}}{FR_{CP}}\right), \qquad \text{(Equation 1)}$$

where FR_{RP} is the mean firing rate during the response period and FR_{CP} is the mean firing rate during the control period. The control period extended from 5 s before the onset of each GABA pulse until the onset of each GABA pulse. Therefore, the FR_{CP} was calculated independently for each pulse. Lastly, we fit the changes in "response to GABA (%)" with the decay curve below to calculate the time necessary to reach 80% of the gabazine effect

$$\text{Response to GABA}\ (\%)(t) = A + Be^{(-rt)}, \qquad \text{(Equation 2)}$$

where "response to GABA(%)(t)" corresponds to the predicted response to GABA (%) at time t, A is the asymptotic value, B the maximum change, and r determines the rate of change.

Monkey

Saccade and pursuit data were sorted based on the direction of eye movement (up and ipsilateral were considered positive; down and contralateral negative). Data collected during the spontaneous saccade task were also sorted into four groups corresponding to ipsilateral (−45–45 deg), contralateral

(135–225 deg), upward (45–135 deg), and downward (225 to −45 deg). PSTHs were constructed from the sorted behavioral and neuronal responses using 2 ms bin size and 17 points moving average smoothing. A 20 deg/s eye velocity threshold was used to determine the onset and offset of each saccade. Saccade gain was calculated as the ratio between saccade amplitude and target movement amplitude. A 30 deg/s^2 acceleration threshold was used to detect the onset of pursuit; this was then manually inspected. Pursuit gain was measured as the ratio between plateau eye velocity (mean desaccaded eye velocity 300–350 ms after pursuit onset) and target eye velocity.

We used a Wilcoxon rank-sum test over the averaged PC data (PSTH; constructed using 2 ms bin size with 17 points moving average) to determine whether or not PCs were responsive to pursuit and saccades. Specifically, we compared the PC firing rate during the control period to that during the response period using a 70-ms moving window that slides in 2-ms steps from the beginning to the end of the response period (Blazquez et al., 2002). A PC was considered responsive if we found significant changes ($p < 0.05$) in firing rate in six consecutive windows. For those eye movement directions where a neuron showed significant response, we quantified PC responses as follows.

PC response to saccades was calculated as the maximum change in firing rate during the response period (−10–180 ms after saccade onset) with respect to the mean firing rate during the control period (100–500 ms before saccade onset). PC responses to saccades took positive values for increases in firing rate and negative values for decreases in firing rate. PCs with positive responses for one or more directions and no negative responses were called ON neurons. PCs with negative responses for one or more directions and no positive responses were called OFF neurons. PCs with positive and negative responses were called ON/OFF neurons. Next, the increase in firing rate (*incFR*) was plotted against each saccade direction (counterclockwise; right = 0; up = 90; left = 180; down = 270) and the data were fitted with a cosine function of the form

$$Saccade\ response(direction) = A + B * \cos(direction), \qquad \text{(Equation 3)}$$

where A is the baseline of the cosine function, which corresponds to the tuning width, and B is the response amplitude (see insets in Figure S1). This function estimates the preferred direction (direction of maximum response), directional tuning (B/A), and tuning width (A).

Sinusoidal pursuit and VOR cancellation data were fitted by a sine function. Neuronal phase was calculated with respect to eye velocity for pursuit and head velocity for VOR cancellation. During VOR cancellation, our monkeys generated minimal eye movements. Only in few cases, where the amplitude of eye movements were >2 deg/s, we subtracted from the PC response the component attributed to eye movement (calculated during pursuit, Lisberger, 1994). PC sensitivities to eye and head velocity during sinusoidal pursuit were calculated as the slope of the fitting line describing the relation between PC firing rate and eye or head velocity. PC responses to step ramp pursuit were quantified using standard methods, specifically the multiple linear regression approach expressed in Equation 4

$$f(t) = \alpha\ddot{E}(t) + \beta\dot{E}(t) + \gamma E(t) + \delta + \epsilon(t), \qquad \text{(Equation 4)}$$

where f(t) is the PC firing rate at time t; α, β, and γ correspond to the PC sensitivities to eye acceleration ($\ddot{E}$), eye velocity ($\dot{E}$), and eye position (E), respectively; δ is the PC baseline firing rate; and ϵ is the error term (Blazquez et al., 2003).

SUPPLEMENTAL INFORMATION

Supplemental Information includes seven figures and can be found with this article online at http://dx.doi.org/10.1016/j.celrep.2015.04.020.

AUTHOR CONTRIBUTIONS

P.M.B. was involved in all aspects of the project, including neuronal recordings, data analysis, and manuscript preparation. T.A.Y. helped with neuronal recordings, interpretation of the data, and manuscript preparation.

ACKNOWLEDGMENTS

We thank Drs. Stephen Highstein, Dora Angelaki, and Harold Barton for equipment and support; Dr. Yutaka Hirata and Shane Heiney for help editing the manuscript; Fanetta Hampton, Valentin Militchin, Krystal Henderson, and Darryl Craig for technical support and animal care; and Keith Graham and Buster Tipton of TORAY Carbon Fiber for supplying the carbon fibers. This work was funded by grants NINDS R01-NS065099 (to P.M.B.), the McDonnell Center for Higher Brain Function (to P.M.B.), NIDCD R03-DC011142 (to T.A.Y.), and NEI R01-EY012814 (to D.E.A.).

Received: November 3, 2014
Revised: January 27, 2015
Accepted: April 7, 2015
Published: May 7, 2015

REFERENCES

Blazquez, P.M., Fujii, N., Kojima, J., and Graybiel, A.M. (2002). A network representation of response probability in the striatum. Neuron *33*, 973–982.

Blazquez, P.M., Hirata, Y., Heiney, S.A., Green, A.M., and Highstein, S.M. (2003). Cerebellar signatures of vestibulo-ocular reflex motor learning. J. Neurosci. *23*, 9742–9751.

Blot, A., and Barbour, B. (2014). Ultra-rapid axon-axon ephaptic inhibition of cerebellar Purkinje cells by the pinceau. Nat. Neurosci. *17*, 289–295.

Cerminara, N.L., Aoki, H., Loft, M., Sugihara, I., and Apps, R. (2013). Structural basis of cerebellar microcircuits in the rat. J. Neurosci. *33*, 16427–16442.

D'Angelo, E. (2014). The organization of plasticity in the cerebellar cortex: from synapses to control. Prog. Brain Res. *210*, 31–58.

De Zeeuw, C.I., Hansel, C., Bian, F., Koekkoek, S.K., van Alphen, A.M., Linden, D.J., and Oberdick, J. (1998). Expression of a protein kinase C inhibitor in Purkinje cells blocks cerebellar LTD and adaptation of the vestibulo-ocular reflex. Neuron *20*, 495–508.

Donaldson, I.M. (2000). The functions of the proprioceptors of the eye muscles. Philos. Trans. R. Soc. Lond. B Biol. Sci. *355*, 1685–1754.

Duguid, I., Branco, T., London, M., Chadderton, P., and Häusser, M. (2012). Tonic inhibition enhances fidelity of sensory information transmission in the cerebellar cortex. J. Neurosci. *32*, 11132–11143.

Eccles, J., Ito, M., and Szentagothai, J. (1967). The cerebellum as a Neuronal Machine (Berlin: Springer-Verlag).

Escudero, M., Cheron, G., and Godaux, E. (1996). Discharge properties of brain stem neurons projecting to the flocculus in the alert cat. II. Prepositus hypoglossal nucleus. J. Neurophysiol. *76*, 1775–1785.

Franklin, K.B.J., and Paxinos, G. (2008). The mouse brain in stereotaxic coordinates (New York: Elsevier Science).

Gao, W., Chen, G., Reinert, K.C., and Ebner, T.J. (2006). Cerebellar cortical molecular layer inhibition is organized in parasagittal zones. J. Neurosci. *26*, 8377–8387.

Ghasia, F.F., Meng, H., and Angelaki, D.E. (2008). Neural correlates of forward and inverse models for eye movements: evidence from three-dimensional kinematics. J. Neurosci. *28*, 5082–5087.

Hansel, C., de Jeu, M.T.G., Belmeguenai, A., Houtman, S.H., Buitendijk, G., Andreev, D., De Zeeuw, C.I., and Elgersma, Y. (2006). alphaCaMKII is essential for cerebellar LTD and motor learning. Neuron *51*, 835–843.

Heine, S.A., Highstein, S.M., and Blazquez, P.M. (2010). Golgi cells operate as state-specific temporal filters at the input stage of the cerebellar cortex. J. Neurosci. *30*, 17004–17014.

Herz, A., Zieglgänsberger, W., and Färber, G. (1969). Microelectrophoretic studies concerning the spread of glutamic acid and GABA in brain tissue. Exp. Brain Res. *9*, 221–235.

Inagaki, K., Heiney, S.A., and Blazquez, P.M. (2009). Method for the construction and use of carbon fiber multibarrel electrodes for deep brain recordings in the alert animal. J. Neurosci. Methods *178*, 255–262.

Isope, P., and Barbour, B. (2002). Properties of unitary granule cell—>Purkinje cell synapses in adult rat cerebellar slices. J. Neurosci. *22*, 9668–9678.

Jirenhed, D.-A., Bengtsson, F., and Jörntell, H. (2013). Parallel fiber and climbing fiber responses in rat cerebellar cortical neurons in vivo. Front. Syst. Neurosci. *7*, 16.

Jörntell, H., and Ekerot, C.F. (2002). Reciprocal bidirectional plasticity of parallel fiber receptive fields in cerebellar Purkinje cells and their afferent interneurons. Neuron *34*, 797–806.

Langer, T., Fuchs, A.F., Chubb, M.C., Scudder, C.A., and Lisberger, S.G. (1985). Floccular efferents in the rhesus macaque as revealed by autoradiography and horseradish peroxidase. J. Comp. Neurol. *235*, 26–37.

Laurens, J., Heiney, S.A., Kim, G., and Blazquez, P.M. (2013). Cerebellar cortex granular layer interneurons in the macaque monkey are functionally driven by mossy fiber pathways through net excitation or inhibition. PLoS One *8*, 12.

Lisberger, S.G. (1994). Neural basis for motor learning in the vestibuloocular reflex of primates. III. Computational and behavioral analysis of the sites of learning. J. Neurophysiol. *72*, 974–998.

Liu, S.J., Lachamp, P., Liu, Y., Savtchouk, I., and Sun, L. (2008). Long-term synaptic plasticity in cerebellar stellate cells. Cerebellum *7*, 559–562.

Miles, F.A., Fuller, J.H., Braitman, D.J., and Dow, B.M. (1980). Long-term adaptive changes in primate vestibuloocular reflex. III. Electrophysiological observations in flocculus of normal monkeys. J. Neurophysiol. *43*, 1437–1476.

Mitchell, S.J., and Silver, R.A. (2003). Shunting inhibition modulates neuronal gain during synaptic excitation. Neuron *38*, 433–445.

Noda, H., and Suzuki, D.A. (1979). The role of the flocculus of the monkey in saccadic eye movements. J. Physiol. *294*, 317–334.

Paxinos, G., Huang, X.-F., and Toga, A.W. (2000). The rhesus monkey brain in stereotaxic coordinates (San Diego: Accademic Press).

Pijpers, A., Apps, R., Pardoe, J., Voogd, J., and Ruigrok, T.J. (2006). Precise spatial relationships between mossy fibers and climbing fibers in rat cerebellar cortical zones. J. Neurosci. *26*, 12067–12080.

Rambold, H., Churchland, A., Selig, Y., Jasmin, L., and Lisberger, S.G. (2002). Partial ablations of the flocculus and ventral paraflocculus in monkeys cause linked deficits in smooth pursuit eye movements and adaptive modification of the VOR. J. Neurophysiol. *87*, 912–924.

Ruskell, G.L. (1999). Extraocular muscle proprioceptors and proprioception. Prog. Retin. Eye Res. *18*, 269–291.

Sato, Y., and Kawasaki, T. (1990). Operational unit responsible for plane-specific control of eye movement by cerebellar flocculus in cat. J. Neurophysiol. *64*, 551–564.

Sato, Y., and Kawasaki, T. (1991). Identification of the Purkinje cell/climbing fiber zone and its target neurons responsible for eye-movement control by the cerebellar flocculus. Brain Res. Brain Res. Rev. *16*, 39–64.

Schonewille, M., Belmeguenai, A., Koekkoek, S.K., Houtman, S.H., Boele, H.J., van Beugen, B.J., Gao, Z., Badura, A., Ohtsuki, G., Amerika, W.E., et al. (2010). Purkinje cell-specific knockout of the protein phosphatase PP2B impairs potentiation and cerebellar motor learning. Neuron *67*, 618–628.

van Alphen, A.M., and De Zeeuw, C.I. (2002). Cerebellar **LTD** facilitates but is not essential for long-term adaptation of the vestibulo-ocular reflex. Eur. J. Neurosci. *16*, 486–490.